Lawrence Berkeley Laboratory
UNIVERSITY OF CALIFORNIA

Materials & Molecular
Research Division

To be published as a chapter in Vibrational Spectroscopies Applied to the Characterization of Adsorbed Species on Catalysts, American Chemical Society, Fall 1980

# THE APPLICATION OF HIGH RESOLUTION ELECTRON ENERGY LOSS SPECTROSCOPY TO THE CHARACTERIZATION OF ADSORBED MOLECULES ON RHODIUM SINGLE CRYSTAL SURFACES

L. H. Dubois and G. A. Somorjai

January 1980



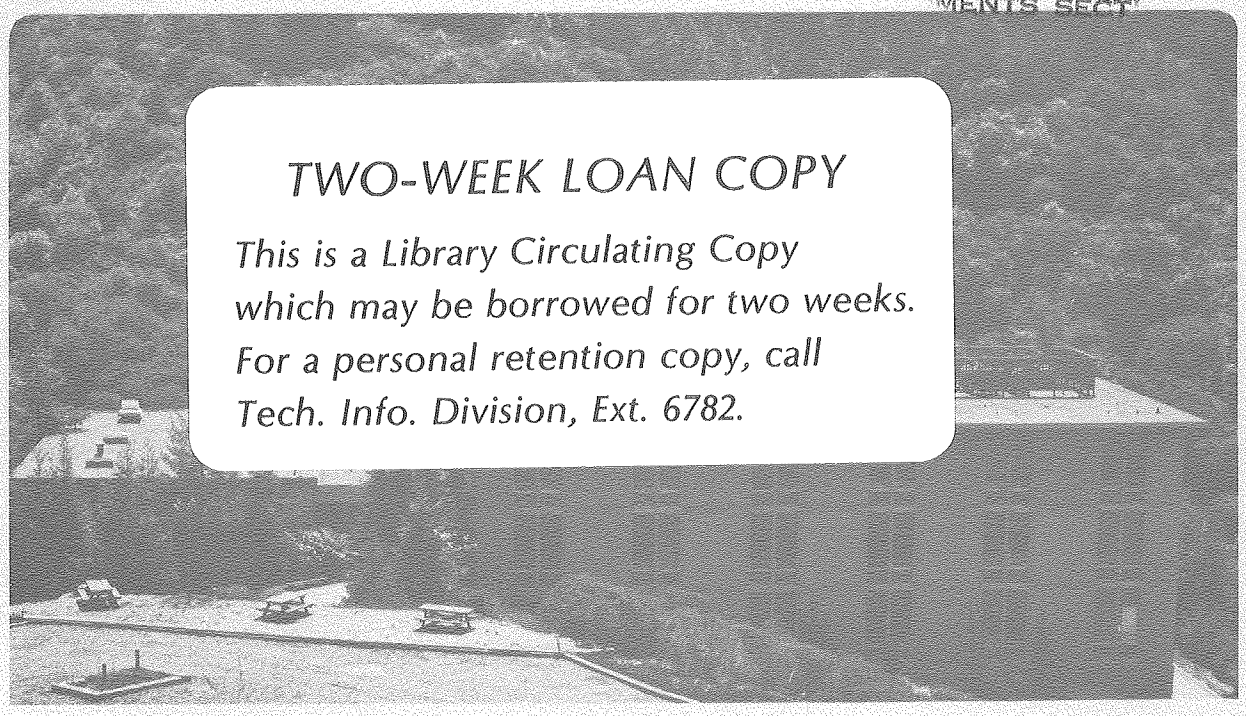



Prepared for the U.S. Department of Energy under Contract W-7405-ENG-48

## DISCLAIMER

# The Application of High Resolution Electron Energy Loss Spectroscopy to the Characterization of Adsorbed Molecules on Rhodium Single Crystal Surfaces

L. H. Dubois and G. A. Somorjai

Materials and Molecular Research Division,
Lawrence Berkeley Laboratory and Department of Chemistry,
University of California, Berkeley, CA 94720

The scattering of low energy electrons by metal surfaces has been studied for many years now (1, 2). The electron's ease of generation and detection and high surface sensitivity (low penetration depth) make it an ideal probe for surface scientists (1, 2). The impinging electron can interact with the surface in basically two ways: it can either elastically reflect (or diffract) from the surface without losing energy or lose a portion of it's incident energy and inelastically scatter. In this paper we will be concerned with only one of many possible inelastic scattering processes: the loss of the electron's energy to the vibrational modes of atoms and molecules chemisorbed on the surface. This technique is known as high resolution electron energy loss spectroscopy (or ELS, EELS, HRELS, HREELS, etc.)

## A. Overview

A.1. The Scattering Process. Evans and Mills (3) and Ibach (4) showed that the photon-surface oscillating dipole and the long range electron-surface oscillating dipole interactions are similar and therefore, to first order, infrared spectroscopy and high resolution ELS provide the same information. Furthermore, due both to the long range nature of this interaction (3, 4) and to the large dielectric constant of the substrate, the same selection rules should apply. Specifically, only vibrational modes which contain an oscillating dipole moment with a component perpendicular to the surface can be excited (3, 4). Sokcevic et al. (5, 6, 7) showed that for ELS this normal dipole selection rule can break down under certain conditions, however. Furthermore, for the case of short range "impact" scattering, both theory and experiment indicate that all possible normal mode vibrations are observed (8, 9, 10). A more detailed discussion of the theory of the inelastic scattering of low energy electrons by surface vibrational modes is presented elsewhere in this volume (11).

The beginning of high resolution electron energy loss spectroscopy can be traced to the pioneering work of F. M. Propst and T. C. Piper in 1967 (12). Credit for the expansion of this technique, however, must be given to Harold Ibach and his graduate students (2, 13) who played a key role in both the advancement of spectrometer design and in the performance of outstanding experiments. At present there are almost a dozen working systems throughout the world and more are being built every month.

To study this very low energy inelastic scattering process in the limit of a long range electron-dipole interaction, a collimated beam of monochromatic electrons is incident on a surface and the energy distribution of the specularly reflected beam is recorded. A typical spectrometer for this type of experiment is shown in Figure 1. Electrons are emitted by a hot tungsten filament and are focused onto the slit of a monochromator by an electrostatic lens system. In our spectrometer the monochromator consists of a 127° cylindrical sector although 180° hemispheres (14, 15, 16) and cylindrical mirror analyzers (17, 18) have also been successfully used as energy dispersing elements. For an excellent review of the various types of electrostatic energy analyzers and their advantages and disadvantages, see reference 19. A monoenergetic beam of electrons is then focussed onto the sample by another series of lenses. A 0.1 to 1 nanoamp beam of electrons reaches the crystal with an incident energy between 2 and 10 eV. The specularly reflected electrons are collected by a pair of lenses and focussed onto the slit of the analyzer. The energy analysis of these inelastically scattered electrons is carried out by a cylindrical sector identical to the monochromator. The electrons are finally detected by a channeltron electron multiplier and the signal is amplified, counted and recorded outside of the vacuum chamber. A typical specularly reflected beam has an intensity of $10^5$ to $10^6$ electrons per second in the elastic channel and a full width at half maximum between 7 and 10 meV (60-80 $cm^{-1}$; 1 meV = 8.065 $cm^{-1}$). Scattering into inelastic channels is between 10 and 1000 electrons per second. In our case the spectrometer is rotatable so that possible angular effects can also be studied. This becomes important for the study of vibrational excitation by short range "impact" scattering (8, 9, 10).

A.2. The Advantages of High Resolution ELS. The advantages of this technique for studying the vibrational spectra of chemisorbed molecules are numerous: a) The entire infrared region of the spectrum (from 300 to 4000 $cm^{-1}$) can be scanned in less than twenty minutes without changing windows or prisms. b) These studies can easily be extended to the visible portion of the electromagnetic spectrum (20). c) For strong scatterers, high resolution ELS is sensitive to less than 0.1% of a monolayer (13), far more sensitive than most other techniques. d) Because of both this surface sensitivity and the nature of the inelastic

scattering process (3, 4, 5, 6, 7), single crystal metal surfaces make ideal targets. Thus, studies can be carried out on clean, well characterized substrates. Furthermore, e) a variety of complementary surface sensitive probes (such as low energy electron diffraction (LEED), Auger electron spectroscopy (AES), thermal desorption mass spectrometry (TDS) and X-ray and ultraviolet photoelectron spectroscopy (XPS and UPS)) can now be applied to the study of a given chemisorption system. Through this combination of techniques located in a single ultra-high vacuum chamber, a complete picture of the structure, bonding and reactivity of adsorbed monolayers can be obtained. f) Unlike some other techniques, both disordered (21) and optically rough (22) surfaces can readily be studied. g) Also, because of this surface sensitivity ELS can be used to detect hydrogen both through its vibration against the substrate and against other adsorbed atoms. Finally, h) due to the low incident beam energies and beam currents, high resolution electron energy loss spectroscopy is a non-destructive technique which can be used to probe the structure of weakly absorbed molecules.

While discussing the advantages of high resolution ELS, mention should be made of two of it's major disadvantages. First, by optical standards the terms "high resolution" are a misnomer since the resolution is limited, at present, to about 60 $cm^{-1}$ (the full width at half maximum of the elastic scattering peak). Peak assignments can be made much more accurately ($\pm 5$ $cm^{-1}$), however. This limits the use of isotopic substitution and the analysis of closely spaced vibrational modes. The second major drawback is that the maximum pressure under which experiments can be carried out is approximately $5 \times 10^{-5}$ torr due to electron-gas collisions inside the spectrometer. High pressure catalytic reactions and chemisorption at the solid-liquid interface cannot be readily studied. Nevertheless, a tremendous number of studies on the adsorption of atoms, diatomic molecules and large hydrocarbons on transition metal surfaces have been performed.

A.3. The Application of High Resolution ELS. In the remainder of this paper we wish to show the power of high resolution ELS by discussing in detail its application to two chemisorption systems. Specifically, we will deal with the adsorption of carbon monoxide on the Rh(111) single crystal surface (23) and the adsorption and subsequent reactions of acetylene and ethylene on Rh(111) (24). The vibrational spectra of chemisorbed CO indicate two distinct binding sites (most likely atop and bridged) whose relative populations and vibrational frequencies are determined as a function of both the substrate temperature and background pressure (coverage). Thermal desorption mass spectroscopic measurements show the bridge bonded CO to have an approximately 4 kcal/mole lower binding energy to the surface than the species located in the atop site and therefore this species can be selectively removed from the rhodium crystal.

Surface pretreatment also has a marked effect on CO adsorption: oxygen and carbon both inhibit carbon monoxide chemisorption and weaken the metal-adsorbate bond strength. Co-adsorbed hydrogen has no observable effects.

Below 270 K vibrational spectroscopic measurements indicate that acetylene chemisorbs on Rh(111) with its C-C bond oriented parallel to the surface forming an approximately $sp^2$ hybridized species. LEED investigations show that both $C_2H_2$ and $C_2H_4$ form metastable (2x2) structures on this surface below 270 K. An irreversible order-order transformation occurs between 270 and 300 K to a stable c(4x2) hydrocarbon overlayer in both cases. High resolution ELS and TDS studies show that the stable species formed from both molecules are identical. Hydrogen addition to chemisorbed acetylene is necessary to complete this conversion, however. The structure of the adsorbed ethylene species does not change during this transformation. This stable hydrocarbon species is identical to the hydrocarbon species formed from the chemisorption of either $C_2H_4$ or $C_2H_2$ and hydrogen on Pt(111) above 300 K. Decomposition of these molecules to surface CH (CD) species occurs on Rh(111) above ~420 K.

B. Experimental

Experiments are carried out in an all stainless steel ultra-high vacuum (UHV) chamber built in two levels. The upper portion contains the standard single crystal surface analysis equipment (four grid LEED/Auger optics, glancing incidence electron gun and quadrapole mass spectrometer). After dosing, the samples are lowered into the high resolution electron energy loss spectrometer by an extended travel precision manipulator. The spectrometer is described in detail above (see Figure 1). The design is similar to that of Froitzheim et al. (25). In the present series of experiments the angle of incidence is fixed at 70° to the surface normal and electrons are collected in the specular direction. The elastic scattering peak has a full width at half maximum between 60 and 100 $cm^{-1}$ and a maximum intensity of 1 x $10^5$ counts per second. The vacuum chamber is lined with layers of $\mu$ metal and silicon-iron shielding to reduce stray magnetic fields. The upper and lower levels are also separated by $\mu$ metal. The base pressure in the system is maintained at 1 x $10^{-10}$ torr with two sputter ion pumps and a titanium sublimation pump.

This combination of techniques allows us to determine the structure of the adsorbed species while on the metal surface and after desorption into the gas phase. Furthermore, molecular rearrangements in the adsorbed overlayer as a function of both the substrate temperature and background pressure can be studied.

The procedures for sample preparation, mounting and cleaning have been described previously (26). Briefly, the rhodium single crystal rod was oriented to $\pm 1/2^{\circ}$ using X-ray back reflection and a 1 mm. thick disc was cut by spark erosion. After mechanical

polishing the sample was spot welded to etched tantalum foil and mounted inside the UHV chamber. The Rh(111) crystal was cleaned by a combination of argon ion bombardment (1000-2000 eV) followed by annealing in vacuum (~900 K) and $O_2/H_2$ cycles to remove carbon, sulfur and boron.

Gas adsorption is studied at pressures between $5 \times 10^{-9}$ and $1 \times 10^{-5}$ torr and at temperatures between 210 and 530 K. Surface structures are observed both with increasing exposure and after the gas is pumped away. Neither gas exposures nor background pressures are corrected for ion gauge sensitivity.

## C. The Chemisorption of CO on Rhodium

C.1. Background. The bonding of carbon monoxide to transition metals is one of the most extensively studied chemisorption systems in surface science (27, 28). The interaction of CO with metal atoms or with clusters of metal atoms is also well studied by inorganic chemists (29, 30, 31). As a result of these detailed investigations of CO, comparisons between surfaces and metal cluster carbonyls can now be made (32, 33, 34). The bonding of carbon monoxide to rhodium is of special interest to us since this metal catalyzes the hydrogenation of CO in both heterogeneous (35, 36) and homogeneous media (37). Because of this importance we chose to explore the high resolution electron energy loss spectrum of carbon monoxide chemisorbed on a Rh(111) single crystal surface (23).

Much effort has gone into understanding the vibrational spectrum of CO chemisorbed on rhodium (38). More than 20 years ago Yang and Garland performed the first infrared studies using highly dispersed rhodium particles supported on an inert alumina substrate (39). They provided convincing evidence for a species of the form $Rh(CO)_2$, a gem dicarbonyl, whose IR spectrum showed a doublet at 2095 and 2027 $cm^{-1}$. The presence of linear (~2060 $cm^{-1}$) and bridge bonded (1925 $cm^{-1}$) forms were also demonstrated. More recent investigations (38, 40, 41, 42, 43, 44) agree extremely well with these early experiments except that the C = O vibration of the multiply coordinated species was found to lie near 1860 $cm^{-1}$ in most cases. Supported rhodium cluster carbonyls of known molecular structure have also been studied and analogous stretching frequencies in the 1800 to 2100 $cm^{-1}$ region were reported (45,46). Substrate absorption below 1000 $cm^{-1}$ masked all Rh-CO vibrations. Both transmission and reflection IR studies employing evaporated rhodium films yield similar results (38). Due to the high density of Rh atoms, no species of the form $Rh(CO)_2$ were formed, however. This is expected to be the case on the (111) surface as well. Weak absorptions between 400 and 575 $cm^{-1}$ were seen and are indicative of metal-absorbate stretching and bending vibrations. Inelastic electron tunneling spectroscopic (IETS) measurements on alumina supported rhodium particles (47, 48, 49) add little new structural information

except that peaks in the 400-600 $cm^{-1}$ region have been definitely assigned to Rh-CO bending and
stretching modes.

C.2. CO Chemisorption on Clean Rh(111) (23). The vibrational spectra of carbon monoxide chemisorbed on Rh(111) at 300 K as a function of exposure are shown in Figure 2. At very low exposures (Less than 0.1 L; 1 L = 1 Langmuir = $10^{-6}$ torr • sec) only one peak at 1990 $cm^{-1}$ is observed in the C ≡ O stretching region and no ordered LEED pattern is found. By comparison with the infrared spectra of relevant organorhodium compounds (50, 51) and with matrix isolated metal carbonyls (52), one can assign this loss to the carbon-oxygen stretching vibration of a linearly bonded species. This peak shifts to higher frequency as the coverage is increased. Possible causes for this include local field effects (53, 54), vibrational coupling (54), dipole-dipole interactions (55) or simply a decrease in the total metal-carbon backbonding due to the increased number of adsorbate molecules (56). Currently one lacks a complete understanding of the changes of the forces involved and the individual effects of each perturbation cannot be completely decoupled. Recent infrared studies on single crystal platinum (57) and copper (58) surfaces have attempted to sort out these effects, but due to the extent of the shift here, a combination of all of these mechanisms is most likely present. A result of these effects is a decrease in the rhodium-carbon stretching frequency and possibly a weakening of the metal adsorbate bond. Figure 2 clearly shows a shift in the rhodium-carbon stretching vibration for this linearly bonded species from 480 $cm^{-1}$ to lower frequency with increasing CO exposure. This is consistent with the weakening of the metal-adsorbate bond observed with increasing gas dosage in CO thermal desorption spectra from the Rh(111) surface (23, 26, 59). No other vibrations corresponding to Rh-C ≡ O bending modes were observed in the specular direction and by invoking the normal dipole selection rule (3, 4) we conclude that the carbon-oxygen bond is oriented perpendicular to the surface.

At larger than 0.4 to 0.5 L CO exposures a small shoulder near 1870 $cm^{-1}$ appears. Again by comparison with relevant model compounds (50, 51, 52), one can assign this peak to the carbon-oxygen stretch of a bridge bonded species. Unlike the loss near 2000 $cm^{-1}$, this peak grows at essentially constant frequency, never varying more than ±5 $cm^{-1}$. By a CO exposure of 1.0 L the rhodium-carbon stretch has significantly broadened. The new low frequency shoulder appearing slightly above 400 $cm^{-1}$ corresponds to the metal-carbon stretch of the bridge bonded species. This weaker bond to the substrate for the new species can be correlated with a low temperature desorption peak appearing at high CO exposures in the TDS spectra of reference 23. These measurements show the bridge bonded CO to have an approximately 4 kcal/mole lower binding energy to the surface than the

species located in the atop site. Again the bridge bonded species is oriented perpendicular to the surface since no bending or asymmetic stretching modes are observed in the specular direction.

The vibrational spectra of CO chemisorbed on Rh(111) as a function of background pressure at 300 K are shown in Figure 3. Once again the carbon-oxygen stretch for the atop site continues to shift to higher frequency as a function of coverage and reaches a limiting value of 2060 to 2070 $cm^{-1}$. The rhodium-carbon stretch of the linear species simultaneously decreases to 420 $cm^{-1}$. The 1870 $cm^{-1}$ loss due to the bridge bonded species remains at a constant frequency with increasing coverage, however. The presence of gem dicarbonyl species cannot be ruled out here due to the limited resolution of ELS, but seem unlikely because of the high density of metal atoms on the (111) surface (38) that would lead to extreme crowding of CO molecules in the dicarbonyl configuration.

The chemisorption of carbon monoxide on Rh(111) is completely reversible. As the background CO in Figure 3 is pumped away the carbon-oxygen stretching vibration for the more weakly bonded bridged species decreases in intensity and the metal-carbon and carbon-oxygen stretching vibrations for the atop site shift back into their original positions. The bridge bonded species can be selectively removed from the substrate by slowly heating the crystal to approximately 360 K in vacuum (23). Finally, no CO decomposition is detected under any of the conditions employed in our experiments ($p \leq 1 \times 10^{-5}$ torr CO, $T \leq 600$ K).

By combining the present ELS studies with previous TDS (23, 26, 59) and LEED (23, 59) experiments we can now present a fairly complete picture of CO chemisorption on Rh(111). At very low exposures a single species is present on the surface located in an atop site ($\nu_{Rh-CO} = 480$ $cm^{-1}$, $\nu_{C\equiv O} = 1990$ $cm^{-1}$). As the coverage increases, the bonding to the surface becomes weaker ($\nu_{Rh-C}$ decreases, $\nu_{C\equiv O}$ increases, TDS peak maximum shifts to lower temperatures) (23, 26, 59). This process continues until an approximately 0.5 L exposure where a $(\sqrt{3}x\sqrt{3})R30^{o}$ LEED pattern is seen and all of the adsorbed CO molecules are linearly bounded to individual rhodium atoms (Figure 4a). This has now been confirmed by a low energy electron diffraction structure analysis (60). Above this coverage a second C ≡ O stretching vibration corresponding to a bridge bonded species is observed ($\nu_{Rh-CO} \simeq$ 400 $cm^{-1}$, $\nu_{C=O} = 1870$ $cm^{-1}$). A "split" (2x2) LEED pattern is seen indicating a loosely packed hexagonal overlayer of adsorbate molecules. This overlayer structure compresses upon further CO exposure. Throughout this intermediate coverage regime there is a mixed layer of atop and bridge bonded CO species and we see a continuous growth of all ELS peaks and a shift in the loss above 2000 $cm^{-1}$. Two peaks are also visible in the TDS spectra with the bridge bonded carbon monoxide having an approximately 4 kcal/mole lower binding energy to the surface than the species located in the atop site. Finally, by a background pressure

of approximately 1 x $10^{-6}$ torr CO at 300 K, a (2x2) LEED pattern forms whose unit cell consists of three carbon monoxide molecules--two atop and one bridged (Figure 4b), in reasonable agreement with the two-to-one peak intensity ratio found in the ELS spectra (Figure 3).

C.3. CO Chemisorption on Pretreated Rh(111) (23). Sexton and Somorjai showed that surface pretreatment had a marked effect on the rate of hydrocarbon formation from $H_2$/CO mixtures over polycrystalline rhodium foils (36): oxidation enhanced the methanation rate while surface carbon inhibited product formation. We studied the effects of hydrogen, oxygen and carbon on the CO on Rh(111) vibrational spectra in the hope of understanding the effects of pre-adsorption. An extensive discussion of these findings is presented in reference 23 and we only summarize our results here. $H_2$ pre-adsorption or post-adsorption on Rh(111) at 300 K had no significant effect on the CO vibrational spectra. Furthermore, no room temperature rhodium-hydrogen stretching vibrations were observed, even at $H_2$ exposures up to several thousand Langmuirs. Finally, no changes were seen after heating the crystal to 600 K in 1 x $10^{-5}$ torr of a 3:1 $H_2$/CO mixture for 30 minutes (61).

Oxygen had a significant effect on the carbon monoxide vibrational spectrum, however. $O_2$ chemisorption on Rh(111) is dissociative at 300 K yielding a single metal-oxygen stretching vibration at 520 $cm^{-1}$ (23) and a second order thermal desorption maximum (26, 62). The formation of bridge bonded carbon monoxide was strongly inhibited in the presence of chemisorbed oxygen and the atop sites seemed to saturate with CO by an exposure of only 1 L. It appeared that pre-adsorbed oxygen blocked some of the surface sites so that CO could not adsorb in many of the atop and bridged positions. Since oxygen is strongly electron withdrawing, the extent of rhodium-carbon backbonding decreased and the C-O stretch shifted approximately 50 $cm^{-1}$ to higher frequency. The strength of the metal-adsorbate bond is determined by the electron density in both the $5\sigma$ and $2\pi^*$ molecular orbitals of carbon monoxide and should therefore decrease as well. Consistent with this was a decrease of at least 30 $cm^{-1}$ in the frequency of the metal-carbon stretching vibration and a lowering of the CO thermal desorption temperature by approximately 40 K (23). He found a smaller CO thermal desorption peak area (23) and this is in agreement with fewer CO molecules on the surface in the presence of chemisorbed oxygen.

The Rh(111) surface was covered with carbon by decomposing 5 x $10^{-7}$ torr of either acetylene or ethylene at 1100 K for 10 minutes and subsequent flashing to 1200 K (23). Pre-adsorbed carbon had a very strong inhibiting effect on carbon monoxide chemisorption. This is the same effect it had on the methanation rate (36). The low inelastic scattering intensity indicated relatively small CO coverages while the broad elastic peak and

high background level were indicative of poor ordering. Consistent with this was a high background intensity in the LEED pattern and a decrease in the CO thermal desorption peak area. The carbon overlayer covered most of the crystal face so that there were only a few sites open for CO chemisorption. There was also an electronic interaction between the carbon overlayer and the adsorbed carbon monoxide molecules, since the vibrational peaks shifted slightly and the maximum CO thermal desorption temperature dropped about 10 K (23).

Thus we may conclude that the pre-adsorption of hydrogen had no effect on CO chemisorption on rhodium while both oxygen and carbon blocked many sites for CO chemisorption and weakened the metal-adsorbate interaction ($\nu_{Rh-C}$ decreased, $\nu_{C\equiv O}$ increased, TDS peak maximum shifted to lower temperature).

C.4. Correlation Between Structure and C ≡ O Vibrational Frequency. The accepted picture of carbon monoxide bonding to metals is by electron transfer from the 5σ orbital of CO to the metallic d orbitals and by backbonding of the metallic electrons into the empty $2\pi^*$ orbital of the adsorbate (38). This scheme has been used by both surface scientists and inorganic chemists to explain the infrared spectra of chemisorbed carbon monoxide and of metal carbonyls. Since the electron density in the CO antibonding orbital is increased, the carbon-oxygen stretching frequency should decrease below the gas phase value of 2143 $cm^{-1}$. Furthermore, as the CO is bound to an increasing number of metal atoms this frequency should drop even further as shown in the IR spectra of model organometallic compounds of known molecular structure (38).

It is generally assumed that species with C-O stretching frequencies above 2000 $cm^{-1}$ correspond to linearly bonded CO, frequencies between about 1850 and 2000 $cm^{-1}$ belong to bridge bonded species and those below approximately 1850 $cm^{-1}$ are for face bridging or three-fold coordination (38). Although, the validity of this rule has not been well tested on single crystal surfaces, some preliminary data to support these divisions has been obtained (see Table I). This correlation of the structure of carbon monoxide (determined by low energy electron diffraction) with the C ≡ O stretching frequency (from both IR and high resolution ELS studies) is very limited at present. Clearly more work needs to be done before any simple interpretation of carbon-oxygen vibrational frequencies can be used to infer the structure of chemisorbed CO. One must also recall that the presence of other either electron donating or withdrawing substituents on the surface can alter the CO electron density and will certainly shift the observed stretching frequencies (23, 69, 70).

Finally, LEED, TDS and UPS studies on the interaction of carbon monoxide with the hexagonally closest packed faces of the group VIII metals show numerous similarities. This is not

true of the vibrational spectroscopic data. These results are sumarized in Table II. CO almost always forms a $(\sqrt{3}x\sqrt{3})R30^{o}$

Table I. Correlation of structure and vibrational frequency for CO chemisorbed on transition metal surfaces.

| Surface | Overlayer Structure | Position from LEED | Vibrational Frequency ($cm^{-1}$) |
|---|---|---|---|
| Ni(100) | c(2x2) | atop (63, 64) | 2069 (17) |
| Cu(100) | c(2x2) | atop (64) | 2079 (65), 2089 (66) |
| Rh(111) | $(\sqrt{3}x\sqrt{3})R30^{o}$ | atop (60) | 2020 (23) |
| Pd(100) | $c(4x2)R45^{o}$ | bridge (67) | 1949 (68), 1903 (67) |

surface structure at low coverages (26, 59, 71-79). This LEED pattern compresses through a number of intermediate steps into a hexagonal closest packed overlayer of carbon monoxide molecules. This is the case despite varying electronic configurations and different metal-metal distances (80). The metal-adsorbate bond energies derived from TDS measurements vary by only ±3 kcal/mole on the surfaces where no CO decomposition is detected (26, 59, 73, 76, 78, 79, 81). Furthermore, the binding energy difference between the $4\sigma$ and $5\sigma$ carbon monoxide molecular orbitals, $\Delta(4\sigma-5\sigma)$, varies by only ±0.3 eV (77, 82-88). The vibrational spectra show tremendous differences, however. Both nickel (89) and palladium (68) form multiply coordinated carbonyl species at low CO exposures and the atop species are only seen at high coverage. The CO chemisorption behavior on Rh(111) (23) and Pt(111) (90, 91) are the opposite: here the atop sites populate first and predominate at low CO exposures. Bridge bonded species begin to form at intermediate coverages. Ruthenium is totally different: only a single carbon-oxygen stretching vibration is present at all coverages (11, 92). The reasons for these differences in the nature of CO bonding to the various transition metal surfaces will have to be explored further in the future.

## D. The Chemisorption of Acetylene and Ethylene on Rh(111) (24)

D.1. Introduction. The structure of acetylene and ethylene adsorbed on transition metal surfaces is of fundamental importance in catalysis. An understanding of the interaction of these simple molecules with metal surfaces may provide information on possible surface intermediates in the catalytic hydrogenation/dehydrogenation of ethylene. High resolution ELS is a particularly useful

Table II. Chemisorption of CO on the group VIII metals.

| Surface | Nearest neighbor distance (Å) (80) | LEED | $E_d$(kcal/mole) | $\Delta(4\sigma-5\sigma)$ | Vibrational Spectra ($cm^{-1}$) $\nu_{M=C}$ | $\nu_{CO}$ | |
|---|---|---|---|---|---|---|---|
| Fe(111) | 2.48 | (1x1) (71)<br>decomposed | 24 (71) | 3.2 (82) | | | |
| Ru(0001) | 2.65 | ($\sqrt{3}$ x$\sqrt{3}$)R30° (72, 73)<br>(2$\sqrt{3}$x2$\sqrt{3}$)R30°<br>(5$\sqrt{3}$x5$\sqrt{3}$)R30° | 28 (73) | 3.1 (83, 84) | 445 | 1984 (92)<br>2080 | |
| Co(0001) | 2.50 | ($\sqrt{3}$x$\sqrt{3}$)R30° (74)<br>hexagonal | 25 (74) | | | | |
| Rh(111) | 2.69 | ($\sqrt{3}$x$\sqrt{3}$)R30° (26, 59)<br>split (2x2)<br>(2x2) | 31 (56, 59) | 3.2 (85) | 480<br>420 | 1990<br>2070 | 1870 (23) |
| Ir(111) | 2.71 | ($\sqrt{3}$x$\sqrt{3}$)R30° (75)<br>(2$\sqrt{3}$x2$\sqrt{3}$)R30°<br>split (2$\sqrt{3}$x2$\sqrt{3}$) | 29.5 (81) | 2.7 (86) | | | |
| Ni(111) | 2.49 | ($\sqrt{3}$x$\sqrt{3}$)R30° (76, 77)<br>c(4x2)<br>($\sqrt{7}$x$\sqrt{7}$)R19.2° | 26 (76) | 2.8 (77) | 400 | 1810<br>1910 | 2050 (89) |
| Pd(111) | 2.75 | ($\sqrt{3}$x$\sqrt{3}$)R30° (78)<br>c(4x2)<br>split (2x2)<br>(2x2) | 30.1 (78) | 3.3 (87) | | 1823<br>1946 | 2092 (68) |
| Pt(111) | 2.77 | ($\sqrt{3}$x$\sqrt{3}$)R30° (79)<br>c(4x2)<br>hexagonal | 28 (79) | 3.0 (88) | 476<br>380 | 2089 | 1856 (90, 91)<br>1872 |

probe for studying the hydrocarbon-metal interaction because of both its sensitivity to hydrogen and its broad spectral range (which includes M-C stretching vibrations, C-C stretching vibrations and C-H stretching and bending vibrations). Here we demonstrate the power of this technique by reviewing the results of a detailed investigation on the chemisorption and reactivity of $C_2H_2$ and $C_2H_4$ on the Rh(111) single crystal surface (24).

D.2. LEED Studies of Acetylene and Ethylene Adsorption on Rh(111). Exposing the clean Rh(111) surface between 230 and 250 K to either $C_2H_2$ or $C_2H_4$ results in the appearance of sharp half order diffraction spots in the LEED pattern from a (2x2) surface structure. The new diffraction spots from the ordered hydrocarbon structures are sensitive to surface coverage. Although the spots are visible after a 1 L gas exposure, they do not become sharp and intense until 1.5 L and then immediately begin disordering above 1.5 L.

A diffraction pattern corresponding to a c(4x2) surface structure can be generated from the (2x2) surface structure without additional hydrocarbon exposure. For adsorbed $C_2H_4$ the transformation occurs in vacuum by slowly warming the crystal to 300 K over the course of several hours. Rapid heating results in the formation of a disorderd c(4x2) structure (broad, diffuse diffraction features and some streaking). For adsorbed $C_2H_2$ even this slow warm-up results in a disordered overlayer. To form a well ordered c(4x2) structure from adsorbed acetylene the crystal is annealed for ~4 minutes at 273 K in 1 x $10^{-8}$ torr of $H_2$ with the mass spectrometer filaments on. These filaments are located approximately 5 cm. from the crystal and provide the surface with a good source of atomic hydrogen (93).

In the transformation from the (2x2) to the c(4x2) structures the orientation and shape of the unit cell change (94), but the areas of the primitive unit cells of these two structures are the same (25 $Å^2$ on Rh(111)). Thus, no variation in the surface coverage occurs. Furthermore, AES shows that the carbon coverage from the (2x2) structures produced during $C_2H_2$ and $C_2H_4$ chemisorption are the same and remain constant during the conversion to the c(4x2) structures (24). Thus, changes in binding site and adsorbate geometry are probably taking place without any change in the adsorbate coverage. The transformation from the (2x2) to the c(4x2) surface structures is irreversible; once the c(4x2) structure forms, the crystal can be cooled to 210 K with no visible changes in the diffraction pattern. The c(4x2) structures can only be altered by heating the crystal above 420 K which causes the surface to irreversibly disorder.

D.3. ELS Studies of Acetylene Chemisorption on Rh(111). The vibrational spectrum of the (2x2) hydrocarbon surface structure formed from the chemisorption of $C_2H_2$ on Rh(111) between 210 and 270 K is shown in Figure 5a. The peak positions and their

relative intensities (95) are listed in Table III. Although some of the peaks are not readily visible in this figure, their positions and intensities are obtained from the analysis of at least

Table III. Vibrational modes for the metastable (2x2) - $C_2H_2$ ($C_2D_2$) species observed on Rh(111) at $T \leq 270$ K (all frequencies in $cm^{-1}$).

| $C_2H_2$ ($C_2D_2$)/Rh(111) | Assignments |
|---|---|
| 3085 (~2320) w<br>2984 (2230) m | C-H (C-D) |
| a. | C-C stretch |
| 887 (686) m<br>706 (565) m | C-H (C-D) bend |
| 323 (~300) w | M-C stretch |

Intensity: s = strong m = medium w = weak

a. Small broad peak in the 1300-1400 $cm^{-1}$ region is observed in several spectra (24).

six spectra. A complete analysis of the low frequency region in this spectrum is hampered by a "spurious background peak" near 800 $cm^{-1}$. This apparent loss, first observed by Froitzheim et al., may be caused by electon reflection from the outer half of the analyzer (25). The dashed lines in Figures 5 through 8 indicate the approximate location and magnitude of this peak. As a result of this experimental artifact, both the position and intensity of all loss features between 650 and 900 $cm^{-1}$ are rather uncertain. Isotopic substitution is of some help in assigning the observed vibrational frequencies to normal modes of the adsorbed species. The ELS spectrum of the (2x2) $C_2D_2$ surface structure is shown in Figure 5b.

The vibrational spectra of the (2x2) acetylene overlayer in Figures 5a and 5b do not change up to 270 K in vacuum. Furthermore, the positions and relative intensities of the observed energy loss peaks are independent of the acetylene exposure (from >0.2 L to <50 L) and, more importantly, are independent of surface order (as determined by observation of the LEED pattern). Thus, using high resolution ELS we conclude that the bonding of the adsorbed molecules do not change upon disordering.

The frequencies of the carbon-hydrogen (carbon-deuterium) stretching vibrations can be used to characterize the state of hybridization of the adsorbed species. Acetylene, $C_2H_2$ ($C_2D_2$), is sp hybridized in the gas phase and has C-H (C-D) stretching vibrations between 3289 and 3374 (2439 and 2701) $cm^{-1}$ (98); ethylene, $C_2H_4$ ($C_2D_4$), is $sp^2$ hybridized and has C-H (C-D) stretching vibrations between 2989 and 3106 (2200 and 2345) $cm^{-1}$ (98); while ethane, $C_2H_6$ ($C_2D_6$), is $sp^3$ hybridized and has C-H (C-D) stretching vibrations between 2896 and 2985 (2083 and 2235) $cm^{-1}$ (98). Thus, the losses at 2980 (2230) and 3085 (~2320) $cm^{-1}$ in Figure 5a and 5b and Table III correspond to the C-H (C-D) stretching vibrations of a molecule near $sp^2$ hybridization. This indicates that the C≡C-H (C≡C-D) bond in adsorbed acetylene is no longer linear. The low frequency mode at 323 $cm^{-1}$ does not shift significantly upon deuteration (~20 $cm^{-1}$) and most likely corresponds to the entire molecule vibrating against the surface. The two largest peaks in the spectrum at 706 and 887 $cm^{-1}$ shift by almost 200 $cm^{-1}$ (to 565 and 686 $cm^{-1}$, respectively) when $C_2D_2$ is chemisorbed and can be assigned to C-H (C-D) bending modes. A more detailed discussion of these mode assignments including reference to the IR spectra of model organometallic compounds is presented in reference 24. We assume the adorbate is oriented with its carbon-carbon axis approximately parallel to the surface since only small, broad peaks (1300 - 1400 $cm^{-1}$) are seen in the C-C stretching region. Observation of such a mode in the specular direction is prohibited by the normal dipole selection rule (3, 4) if the C≡C bond is parallel to the surface. The vibrational mode assignments are summarized in Table III.

Bond lengths, bond angles and the position of adsorbed $C_2H_2$ on the surface cannot be accurately determined without a complete dynamical LEED intensity analysis. Nevertheless, the high resolution ELS results indicate that acetylene chemisorbs on Rh(111) below 270 K with its C≡C axis oriented approximately parallel to the surface. The molecule is near $sp^2$ hybridization and therefore the C≡C-H bond angle is no longer linear. A similar $C_2H_2$ geometry is seen in numerous organometallic cluster compounds (33, 34).

Both LEED and ELS indicate that the (2x2) acetylene overlayer is stable on the surface in vacuum between 210 and 270 K. The addition of $H_2$ to adsorbed $C_2H_2$ below ~260 K causes no changes in the observed ELS spectra, although this surface species is still quite reactive. The addition of $H_2$ to chemisorbed $C_2D_2$ below 260 K results in a complex vibrational spectrum with peaks in both the C-H and C-D stretching and bending regions. Although the deuterium and hydrogen readily exchange, no change in the adsorbate geometry is detected by high resolution ELS. The vibrational spectra of adsorbed acetylene only begin to change when the crystal is heated above 270 K in vacuum. The (2x2)-$C_2H_2$ surface structure also disorders at this temperature.

The vibrational spectrum from the c(4x2) acetylene overlayer is shown in Figure 5c. This spectrum can either be obtained by

warming the (2x2) acetylene overlayer to ~270 K in the presence of 1 x $10^{-8}$ torr of hydrogen or by chemisorbing $C_2H_2$ on Rh(111) above 300 K. Hydrogen addition to the surface species above 270 K is necessary to obtain good quality, intense ELS spectra, however. Hydrogen addition was also required to complete this conversion in the LEED studies. This species is stable on the surface up to ~240 K. The structure of this hydrocarbon overlayer will be discussed in more detail in the next section.

D.4. ELS Studies of Ethylene Chemisorption on Rh(111). The vibrational spectra from the (2x2) and c(4x2) ethylene surface structures are shown in Figures 6a and 6b. The ELS spectrum in Figure 6a is obtained by chemisorbing $C_2H_4$ on the crystal below 270 K. Spectrum 6b can either be observed by slowly warming the (2x2) overlayer structure (6a) to room temperature or by simply adsorbing ethylene on the Rh(111) surface above 290 K. Small peaks in the 1800 to 2100 $cm^{-1}$ region are due to background CO adsorption (23). Once again the observed vibrational frequencies are independent of surface order and hydrocarbon exposure (<0.2 to >50 L). Note that these ELS spectra are almost identical to the vibrational spectrum from the stable c(4x2) acetylene overlayer shown in Figure 5c. The hydrocarbon species derived from ethylene chemisorption is also stable on the surface up to ~420 K. Degradation of both the c(4x2) LEED pattern and of the vibrational spectrum occur at this temperature.

The ELS spectrum resulting from the chemisorption of either $C_2H_4$ or $C_2H_2$ and $H_2$ on Pt(111) above room temperature are quite similar (93, 99). This species is similar to the hydrocarbons species obtained from the adsorption of ethylene on Rh(111). This is clearly shown in Figure 7. Although the chemisorption of ethylene on Pt(111) has been studied by numerous techniques (93, 99, 100, 101, 102, 103), there is still debate over the precise geometry of the stable surface species. Proposed structures include ethylidyne (≡C-$CH_3$) (100, 101), ethylidene (>CH-$CH_3$) (93, 99), and a vinyl species (>CH-$CH_2$-) (102, 103). We simply point out that the stable hydrocarbon overlayer formed from the chemisorption of either ethylene or acetylene and hydrogen on both Pt(111) and Rh(111) yield identical vibrational spectra (Figure 7). A more complete discussion of the similarities between the chemisorption of ethylene on Rh(111) and Pt(111) is presented elsewhere (24).

It is interesting to note that the geometry of the adsorbed ethylene species on Rh(111) remains the same (as indicated by the ELS spectra) while the overlayer structure changes from a (2x2) to a c(4x2). Although this conversion is not affected by the presence of hydrogen, H-D exchange will occur in the hydrocarbon overlayer when $H_2$ is added to chemisorbed $C_2D_4$. No change in the adsorbate geometry is detected by high resolution ELS.

The stable ethylene or acetylene plus hydrogen overlayer on Rh(111) can be decomposed to surface CH (CD) species above ~420 K.

The ELS spectra for these two hydrocarbon fragments are shown in Figure 8. Assignment of the observed vibrational frequencies is discussed in detail by Demuth and Ibach for the decomposition of acetylene on Ni(111) (104). It is possible that species such as these are important surface intermediates under high pressure catalytic conditions (105, 106). Further studies in this area are in progress.

D.5. Summary. These investigations lead to the following conclusions:

1. The chemisorption of acetylene and ethylene on Rh(111) yields a series of ordered structures:

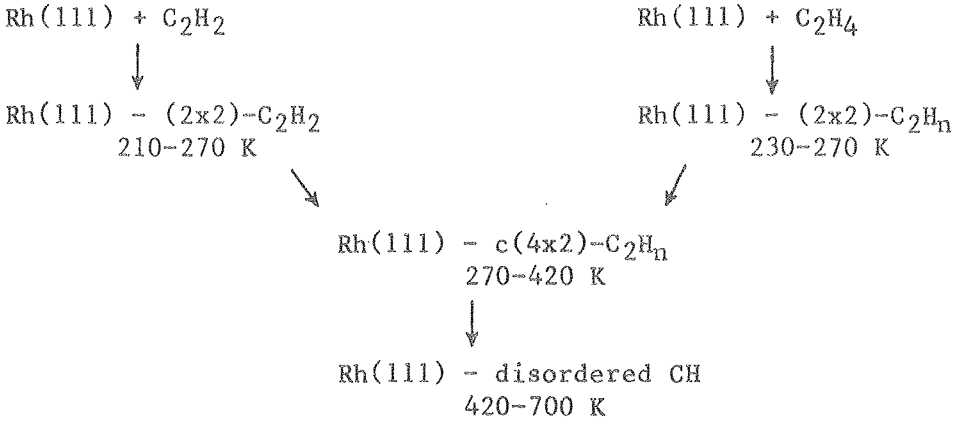


where $C_2H_n$ stands for the stable hydrocarbon species with undetermined hydrogen content. These order-order transformations are irreversible.

2. Below 270 K acetylene chemisorbs on Rh(111) with its C≡C bond oriented parallel to the surface forming an approximately $sp^2$ hybridized species.

3. Adsorption of $C_2H_2$ + H or $C_2H_4$ above 300 K on Rh(111) produces the same stable species. TDS studies show this species to have a stoichiometry of $C_2H_n$, where n is less than 4 (24). Adsorption of $C_2H_2$ + H or $C_2H_4$ on Pt(111) above 350 K leads to a similar, and most likely identical, species.

4. The geometry of the adsorbed ethylene species on Rh(111), as determined by ELS, does not change during the conversion from the metastable to the stable species although the overlayer structure changes from a (2x2) to a c(4x2).

5. The addition of $H_2$ to chemisorbed $C_2D_2$ or $C_2D_4$ results in H-D exchange, but no change in the adsorbate geometry is detected by ELS.

## E. Conclusion

In this paper we have presented several applications of high resolution electron energy loss spectroscopy to the characteriza-

tion of adsorbed molecules on single crystal surfaces. ELS is clearly a very powerful technique for studying the vibrational spectra of chemisorbed molecules. However, no single surface sensitive probe alone can yield a complete picture of the structure, bonding and reactivity of adsorbed species. Experiments utilizing a combination of complementary surface sensitive techniques, in particular ELS and LEED, will yield more detailed structural information about adsorbed atoms and molecules in the future.

Acknowledgments

We thank Prof. P. K. Hansma and Dr. D. G. Castner for many enlightening discussions and for valuable technical assistance. This work was supported by the Division of Materials Science, Office of Basic Energy Sciences, U.S. Department of Energy.

Literature Cited

1. Ertl, G.; Kuppers, J. "Low Energy Electrons and Surface Chemistry," Verlag Chemie: Germany, 1974.
2. Ibach, H., Ed. "Electron Spectroscopy for Surface Analysis," Springer-Verlag: Berlin, 1977.
3. Evans, E.; Mills, D. L. Phys. Rev., 1972, B5, 4126.
4. Ibach, H. Surface Sci., 1977, 66, 56.
5. Sokcevic, D.; Lenac, Z.; Brako, R.; Sunjic, M. Z. Physik., 1977, B28, 273.
6. Sunjic, M.; Brako, R., Lenac, Z.; Sokcevic, D. Intern. J. Quantum Chem., 1977, Suppl. 2, 59.
7. Lenac, Z.; Sunjic, M.; Sokcevic, D.; Brako, R. Surface Sci., 1979, 80, 602.
8. Davenport, J. W.; Ho, W.; Schrieffer, J. R. Phys. Rev., 1978, B17, 3115.
9. Ho, W.; Willis, R. F; Plummer, E. W. Phys. Rev. Letters, 1978, 40, 1463.
10. Willis, R. F.; Ho, W.; Plummer, E. W. Surface Sci., 1979, 88, 384.
11. See chapter by P. A. Thiel and W. H. Weinberg and references therein.
12. Propst, F. M.; Piper, T. C. J. Vac. Sci. Technol., 1967, 4, 53.
13. Ibach, H. "Proceedings of the Conference on Vibrations in Adsorbed Layers," Julich, Germany, 1978; p. 64 and references therein.
14. Dalmai-Imelik, G.; Bertolini, J. C.; Rousseau, J. Surface Sci., 1977, 63, 67.
15. Backx, C.; Feuerbacher, B.; Fitton, B.; Willis, R. F. Surface Sci., 1977, 63, 193.
16. Thomas, G. E.; Weinberg, W. H. Rev. Sci. Instrum., 1979, 50, 497.

17. Andersson, S. Solid State Commun., 1977, 21, 75.
18. Andersson, S. Surface Sci., 1979, 79, 385.
19. Roy, D.; Carette, J. D. in Ibach, H., Ed. "Electron Spectroscopy for Surface Analysis," Springer-Verlag: Berlin, 1977; p. 13.
20. Froitzheim, H.; Ibach, H.; Mills, D. L. Phys. Rev., 1975, B11, 4980.
21. Adnot, A. "Proceedings of the Conference on Vibrations in Adsorbed Layers," Julich, Germany, 1978; p. 109.
22. Dubois, L. H.; Hansma, P. K.; Somorjai, G. A., to be published.
23. Dubois, L. H.; Somorjai, G. A. Surface Sci., 1980, 91, 514.
24. Dubois, L. H.; Castner, D. G.; Somorjai, G. A. J. Chem. Phys., 1980, 72, 000.
25. Froitzheim, H.; Ibach, H.; Lehwald, S. Rev. Sci. Instrum. 1975, 46, 1325.
26. Castner, D. G.; Sexton, B. A.; Somorjai, G. A. Surface Sci. 1978, 71, 519.
27. Ford, R. R. Advan. Catalysis, 1970, 51, 21.
28. Bradshaw, A. M., Surface Sci., 1979, 80, 215.
29. King, R. B. Prog. Inorg. Chem., 1972, 15, 287.
30. Chini, P.; Longini, G.; Albano, V. G. Adv. Organomet. Chem., 1976, 14, 285.
31. Ozin, G. A. Acc. Chem. Res., 1977, 10, 21.
32. Muetterties, E. L. Bull. Soc. Chim. Belg., 1975, 84, 959.
33. Muetterties, E. L. Bull. Soc. Chim. Belg., 1976, 85, 451.
34. Muetterties, E. L.; Rhodin, T. N.; Band, E.; Brucker, C. F.; Pretzer, W. R. Chem. Rev., 1979, 79, 91.
35. Bhasin, M. M.; Bartley, W. J.; Ellgen, P. C.; Wilson, T. P. J. Catal., 1978, 54, 120.
36. Sexton, B. A.; Somorjai, G. A. J. Catal., 1977, 46, 167.
37. Pruett, R. L. Ann. N. Y. Acad. Sci., 1977, 295, 239.
38. See Sheppard, N.; Nguyen, T. T. in Clark, R. J. H.; Hester, R. E., Eds. "Advances in Infrared and Raman Spectroscopy" Vol. 5, Heydon and Son: London, 1978; p. 67 and references therein.
39. Yang, A. C.; Garland, C. W. J. Phys. Chem. 1957, 61, 1504.
40. Arai, H.; Tominaga, H. J. Catal., 1976, 43, 131.
41. Yao, H. C.; Rothschild, W. G. J. Chem. Phys., 1978, 68, 4774.
42. Primet, M. J. C. S. Faraday I, 1978, 74, 2570.
43. Yates, J. T., Jr.; Duncan, T. M.; Worley, S. D.; Vaughn, R. W. J. Chem. Phys., 1979, 70, 1219.
44. Yates, D. J. C.; Murrell, L. L.; Prestridge, E. B. J. Catal., 1979, 57, 41.
45. Smith, G. C.; Chojnacki, T. P.; Drasgupta, S. R.; Iwatata, K.; Watters, W. L. Inorg. Chem., 1975, 14, 1419.
46. Conrad, H.; Ertl, G.; Knozing, H.; Kuppers, J.; Latta, E. E. Chem. Phys. Lett., 1976, 42, 115.

47. Hansma, P. K.; Kaska, W. C.; Laine, R. M. J. Amer. Chem. Soc., 1976, 98, 6064.
48. Klein, J.; Leger, A.; de Cheveigne, S.; Guinet, C.; Belin, M.; Defourneau, D. Surface Sci., 1979, 82, L288.
49. Kroeker, R. M.; Kaska, W. C.; Hansma, P. K.; J. Catal., 1979, 57, 72.
50. Whyman, R. J. C. S. Chem. Comm., 1970, 1194.
51. Griffith, W. P.; Wickam, A. J. J. Chem. Soc. A, 1969, 834.
52. Hanlan, L. A.; Ozin, G. A. J. Amer. Chem. Soc., 1974, 96, 6324.
53. Roth, J. G.; Dignam, M. J. Can. J. Chem., 1976, 54, 1388.
54. Moskovitz, M.; Hulse, J. W. Surface Sci., 1978, 78, 397.
55. Scheffler, M. Surface Sci., 1978, 78, 397.
56. Blyholder, G. J. Phys. Chem., 1964, 68, 2772.
57. Crossley, A.; King, D. A. Surface Sci., 1977, 68, 528.
58. Hollins, P.; Pritchard, J. Surface Sci., 1979, 89, 486.
59. Thiel, P. A.; Williams, E. D.; Yates, J. T., Jr.; Weinberg, W. H. Surface Sci., 1979, 84, 54.
60. Van Hove, M. A.; Koestner, R. J.; Somorjai, G. A., to be published.
61. The Rh(111) surface is catalytically active for Fischer-Tropsch synthesis, but at pressures above one atmosphere (Castner, D. G.; Blackadar, R. L.; Somorjai, G. A., submitted to J. Catal.).
62. Thiel, P. A.; Yates, J. T., Jr.; Weinberg, W. H. Surface Sci., 1979, 82, 22.
63. Passler, M.; Ignatiev, A.; Jona, F.; Jepsen, D. W.; Marcus, P. M. Phys. Rev. Lett., 1977, 43, 360.
64. Andersson, S.; Pendry, J. B. Phys. Rev. Lett., 1977, 43, 363.
65. Horn, K.; Pritchard, J. Surface Sci., 1976, 55, 701.
66. Sexton, B. A., Chem. Phys. Lett., 1979, 63, 451.
67. Behm, R. J.; Christmann, K.; Ertl, G.; Van Hove, M. A.; Thiel, P. A.; Weinberg, W. H. Surface Sci., 1979, 88, L59.
68. Bradshaw, A. M.; Hoffman, F. M. Surface Sci. 1978, 72, 513.
69. Wojtczak, J.; Queau, R.; Poilblane, R. J. Catal., 1975, 37, 391.
70. Ibach, H.; Somorjai, G. A. Appl. Surface Sci., 1979, 3, 293.
71. Yoshida, K.; Somorjai, G. A. Surface Sci., 1978, 75, 46.
72. Williams, E. D.; Weinberg, W. H. Surface Sci., 1979, 82, 93.
73. Madey, T. E.; Menzel, D. Japan J. Appl. Phys. Supp. 2, Part 2, 1974, 229.
74. Bridge, M. E.; Comrie, C. M.; Lambert, R. M.; Surface Sci., 1977, 67, 393.
75. Kuppers, J.; Plagge, A. J. Vac. Sci. Technol., 1976, 13, 259.

76. Christmann, K.; Schober, O.; Ertl, G. J. Chem. Phys., 1974, 60, 4719.
77. Conrad, H.; Ertl, G.; Kuppers, J.; Latta, E. E. Surface Sci., 1976, 57, 475.
78. Conrad, H.; Ertl, G.; Koch, J.; Latta, E. E. Surface Sci., 1974, 43, 462.
79. Ertl, G.; Neumann, M.; Streitt, K. M. Surface Sci, 1977, 64, 393.
80. Kittel, C. "Introduction to Solid State Physics," Wiley, New York, 1976; p. 32.
81. Nieuwenhuys, B. E.; Hagen, D. I.; Rovida, G.; Somorjai, G. A. Surface Sci. 1976, 59, 155.
82. Textor, H. M.; Gay, I. D.; Mason, R. Proc. Royal Soc. London, Ser. A., 1977, 356, 37.
83. Fuggle, J. C.; Madey, T. E.; Steinkilberg, M.; Menzel, D. Phys. Lett. 1975, 51A, 163.
84. Fuggle, J. C.; Madey, T. E.; Steinkilberg, M.; Menzel, D. Surface Sci., 1975, 52, 521.
85. Braun, W.; Neumann, M.; Iwan, M.; Koch, E. E. Solid State Commun., 1978, 27, 155.
86. Zhdan, P. A.; Boreskov, G. K.; Baronin, A. I.; Egelhoff, W. F., Jr.; Weinberg, W. H. Chem. Phys. Lett., 1976, 44, 528.
87. Lloyd, D. R.; Quinn, C. M.; Richardson, N. V. Solid State Commun. 1976, 20, 409.
88. Iwasawa, Y.; Mason, R.; Textor, M.; Somorjai, G. A. Chem. Phys. Lett., 1976, 44, 468.
89. Erley, W.; Wagner, H.; Ibach, H. Surface Sci., 1979, 80, 612.
90. Froitzheim, H.; Hopster, H.; Ibach, H.; Lehwald, S. Appl. Phys. 1977, 13, 147.
91. Hopster, H.; Ibach, H. Surface Sci., 1978, 77, 109.
92. Thomas, G. E.; Weinberg, W. H.; J. Chem. Phys., 1979, 70, 1437.
93. Ibach, H.; Lehwald, S. J. Vac. Sci. Technol., 1978, 15, 407.
94. On the (111) crystal face of an fcc metal the (2x2) unit cell is a rhombohedron while the c(4x2) primitive unit cell is a rectangle.
95. The loss intensities are a strong function of the incident electron energy and only average values are reported here. This could be due to molecular resonances or short range "impact" scattering (8, 9, 10, 96) as discussed by Lehwald and Ibach for the case of acetylene chemisorbed or Ni(111) (97).
96. Andersson, S.; Davenport, J. W. Solid State Commun., 1978, 28, 677.
97. Lehwald, S.; Ibach, H.; to be published.

98. See for example, Shimanouchi, T. "Tables of Molecular Vibrational Frequencies," consolidated Vol. 1, U.S. Department of Commerce publication NSROS-NBS 39, 1972.
99. Ibach, H.; Hopster, H.; Sexton, B. Appl. Surface Sci., 1977, 1, 1.
100. Kesmodel, L. L.; Dubois, L. H.; Somorjai, G. A. Chem. Phys. Lett. 1978, 56, 267.
101. Kesmodel, L. L.; Dubois, L. H.; Somorjai, G. A. J. Chem. Phys., 1979, 70, 2180.
102. Demuth, J. E. Surface Sci., 1979, 80, 367.
103. Demuth, J. E. Surface Sci., to be published.
104. Demuth, J. E.; Ibach, H. Surface Sci., 1978, 78, L238.
105. Hattori, T.; Burwell, R. L. Jr. J. Phys. Chem., 1979, 83, 241.
106. Davis, S. M.; Somorjai, G. A., to be published.

Figure Captions

1. Schematic diagram of the high resolution electron energy loss spectrometer used in these studies. The dispersive elements are 127° cylindrical sectors.

2. Vibrational spectra of CO chemisorbed on an initially clean Rh(111) single crystal surface at 300 K as a function of gas exposure. Note the shift in both the 480 and 1990 $cm^{-1}$ losses with increasing surface coverage.

3. Vibrational spectra of CO chemisorbed on Rh(111) at 300 K as a function of background gas pressure. The loss above 2000 $cm^{-1}$ reaches a limiting value of 2070 $cm^{-1}$ while the peak at 1870 $cm^{-1}$ increases in intensity at a constant frequency.

4. Real space representations of carbon monoxide chemisorbed on a Rh(111) surface: (a) $(\sqrt{3}x\sqrt{3})R30^{o}$ overlayer structure visible at low CO exposures; (b) (2x2) structure seen at high surface coverage.

5. High resolution ELS spectra of chemisorbed acetylene on Rh(111). (a) (2x2)-$C_2H_2$; (b) (2x2)-$C_2D_2$ and (c) c(4x2)-$C_2H_2$ + H. The vibrational assignments for spectra (a) and (b) are listed in Table III. Spectrum (c) is discussed in more detail in the next section.

6. High resolution ELS spectra of chemisorbed ethylene on Rh(111). (a) (2x2) from $C_2H_4$ chemisorption; (b) c(4x2) from $C_2H_4$ chemisorption and (c) (2x2) from $C_2D_4$ chemisorption.

7. Comparison of the vibrational spectra for ethylene chemisorbed on (a) Pt(111) (93) and (b) Rh(111) (24). A discussion of the similarities between acetylene and ethylene chemisorption on Rh(111) and Pt(111) is presented in reference 24.

8. CH (CD) species can be formed on Rh(111) by heating chemisorbed (a) $C_2H_2$ or (b) $C_2D_4$ to 450 K. The peak assignments are discussed in reference 104.

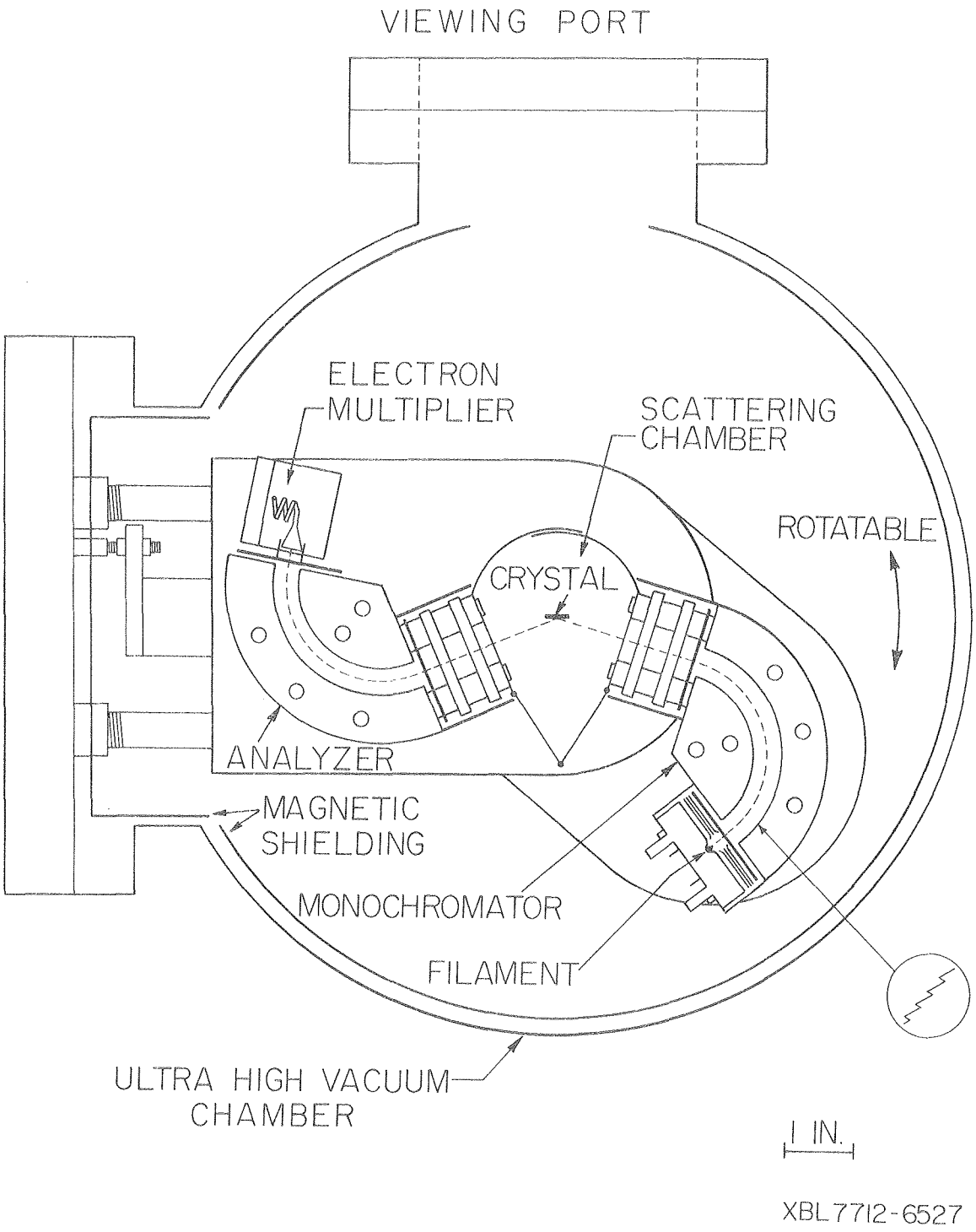
VIEWING PORT
ELECTRON MULTIPLIER
SCATTERING CHAMBER
ROTATABLE
CRYSTAL
ANALYZER
MAGNETIC SHIELDING
MONOCHROMATOR
FILAMENT
ULTRA HIGH VACUUM CHAMBER
1 IN.
XBL7712-6527

Fig.1

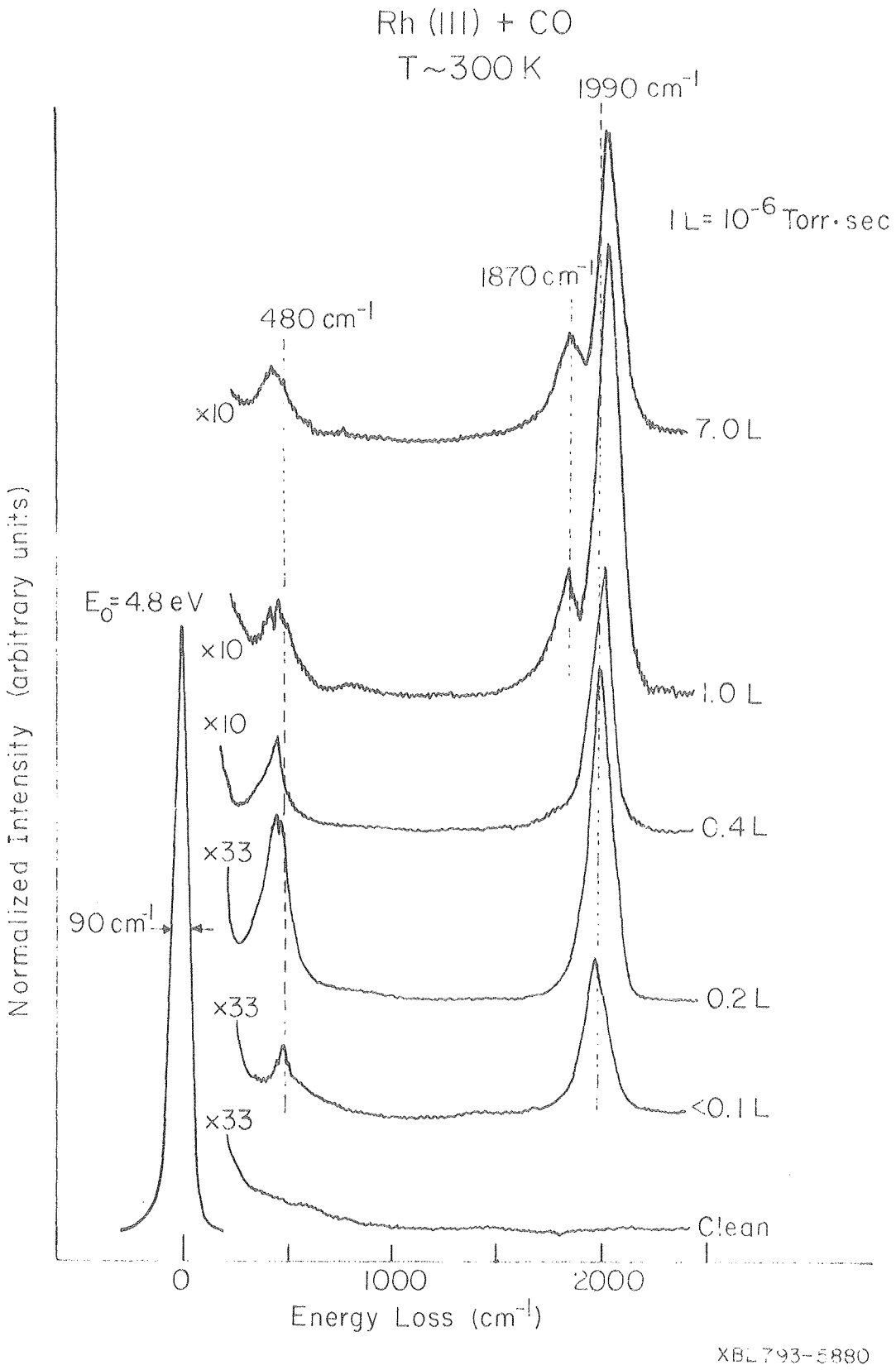


XBL793-5880

Fig. 2

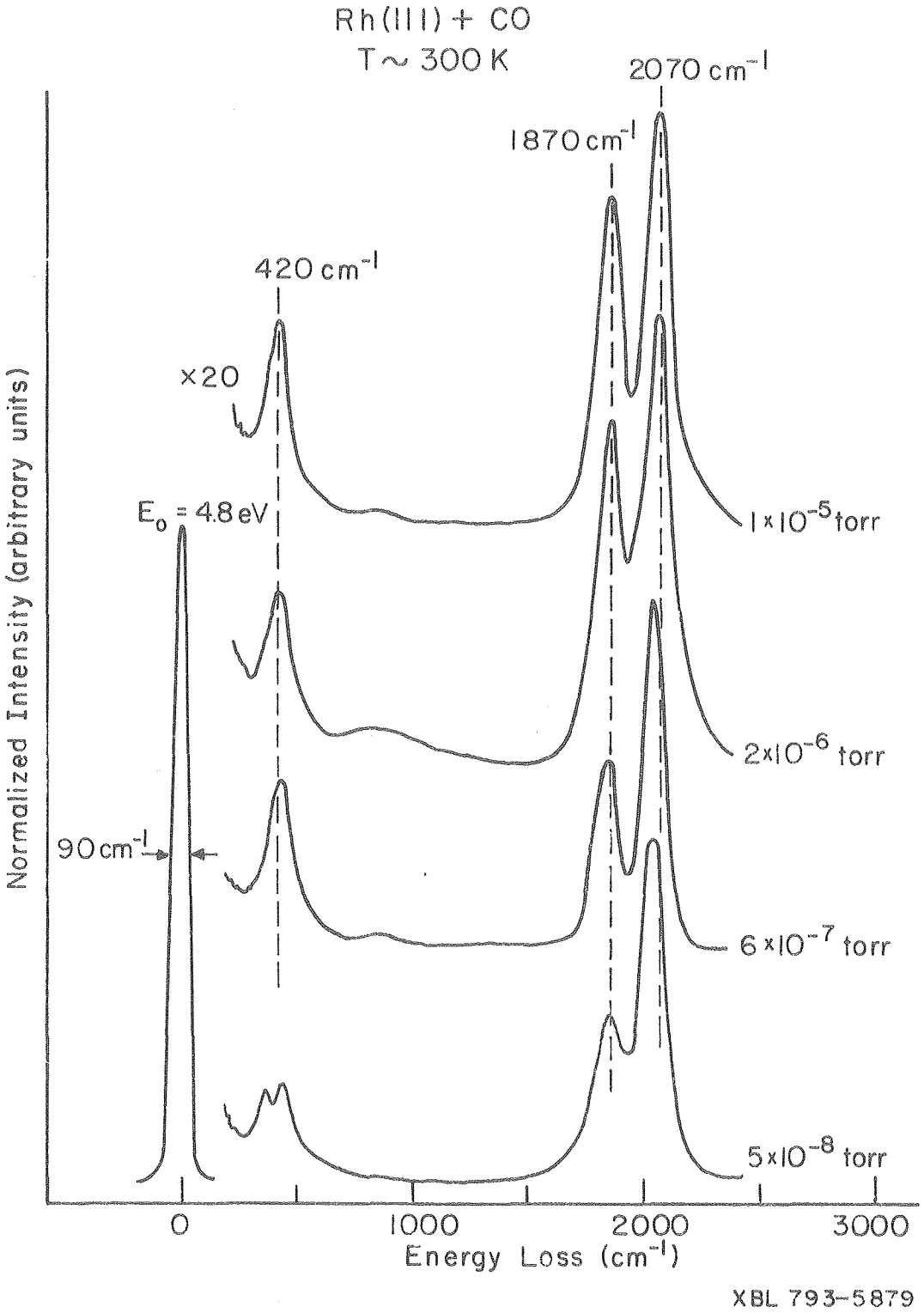
Rh(111) + CO
T ~ 300 K
2070 cm⁻¹
1870 cm⁻¹
420 cm⁻¹
×20
E₀ = 4.8 eV
90 cm⁻¹
1×10⁻⁵ torr
2×10⁻⁶ torr
6×10⁻⁷ torr
5×10⁻⁸ torr
Normalized Intensity (arbitrary units)
0
1000
2000
3000
Energy Loss (cm⁻¹)
XBL 793-5879

Fig.3

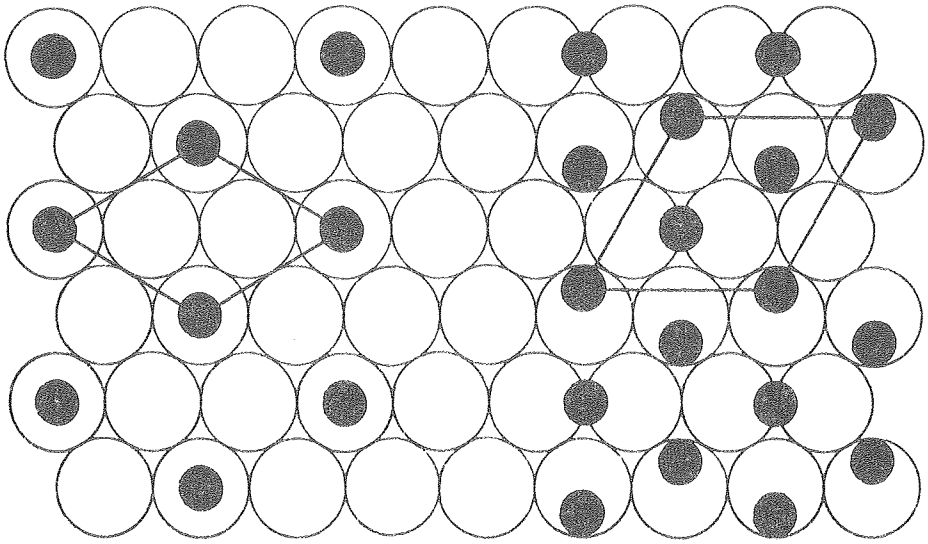

$(\sqrt{3} \times \sqrt{3})R30$ $\quad$ $(2 \times 2)$

$\theta = 1/3$ $\quad$ $\theta = 3/4$

a. $\quad$ b.

XBL795-6248

Fig.4

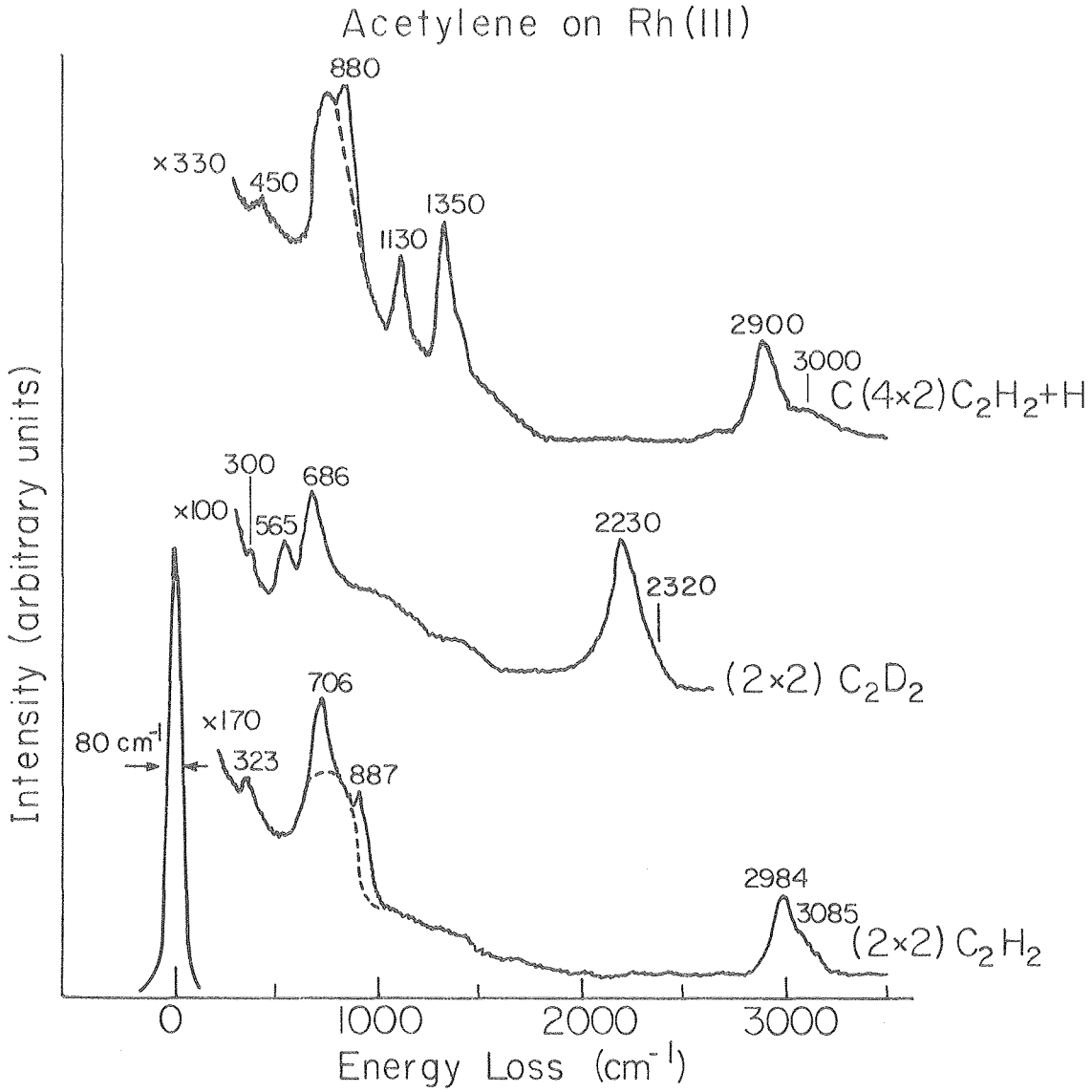


XBL798-6968

Fig.5

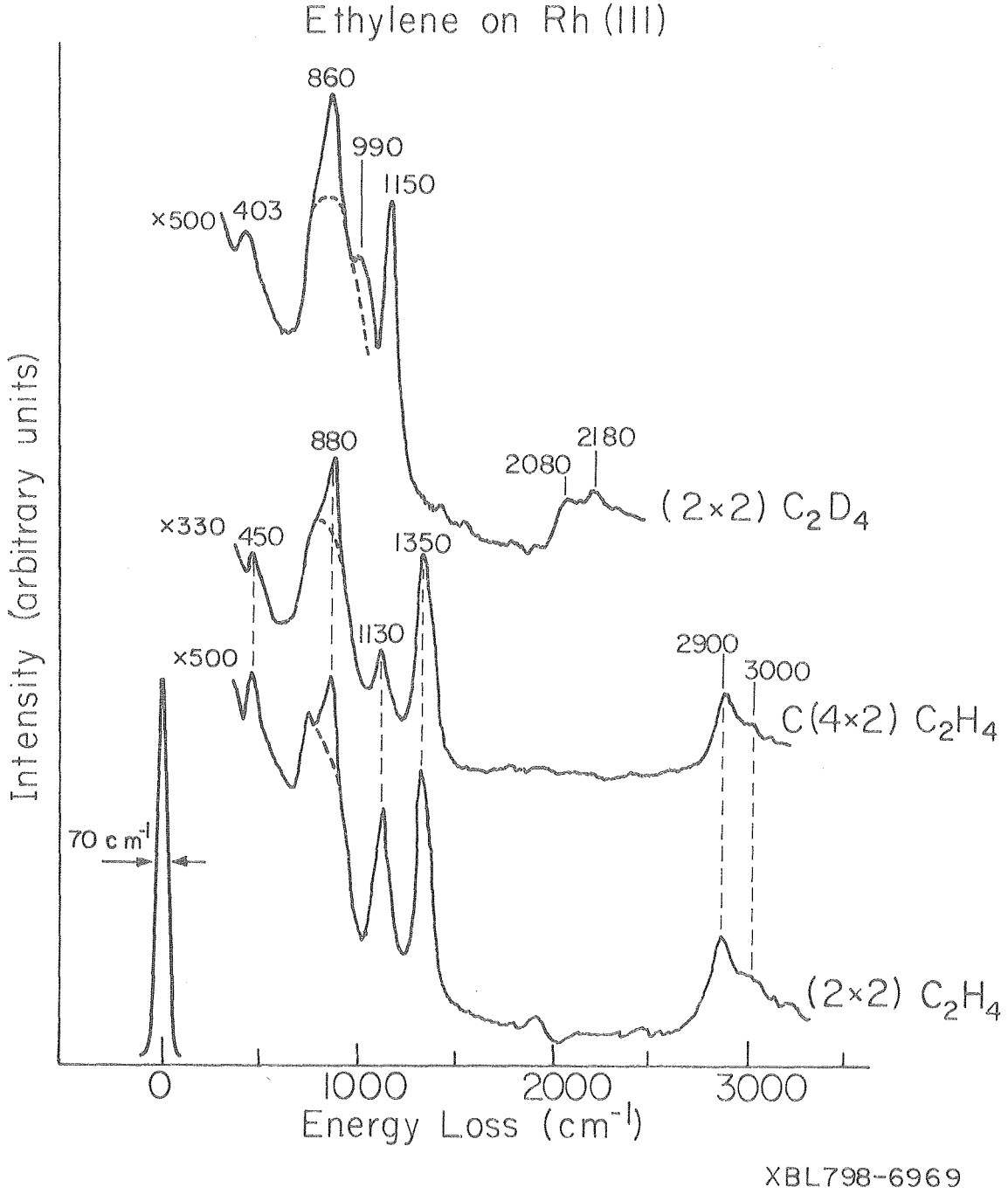
Ethylene on Rh (111)
860
990
1150
×500
403
880
2180
2080
(2×2) C2D4
×330
450
1350
1130
2900
3000
×500
C(4×2) C2H4
70 cm-1
(2×2) C2H4
Intensity (arbitrary units)
0
1000
2000
3000
Energy Loss (cm-1)
XBL798-6969

Fig.6

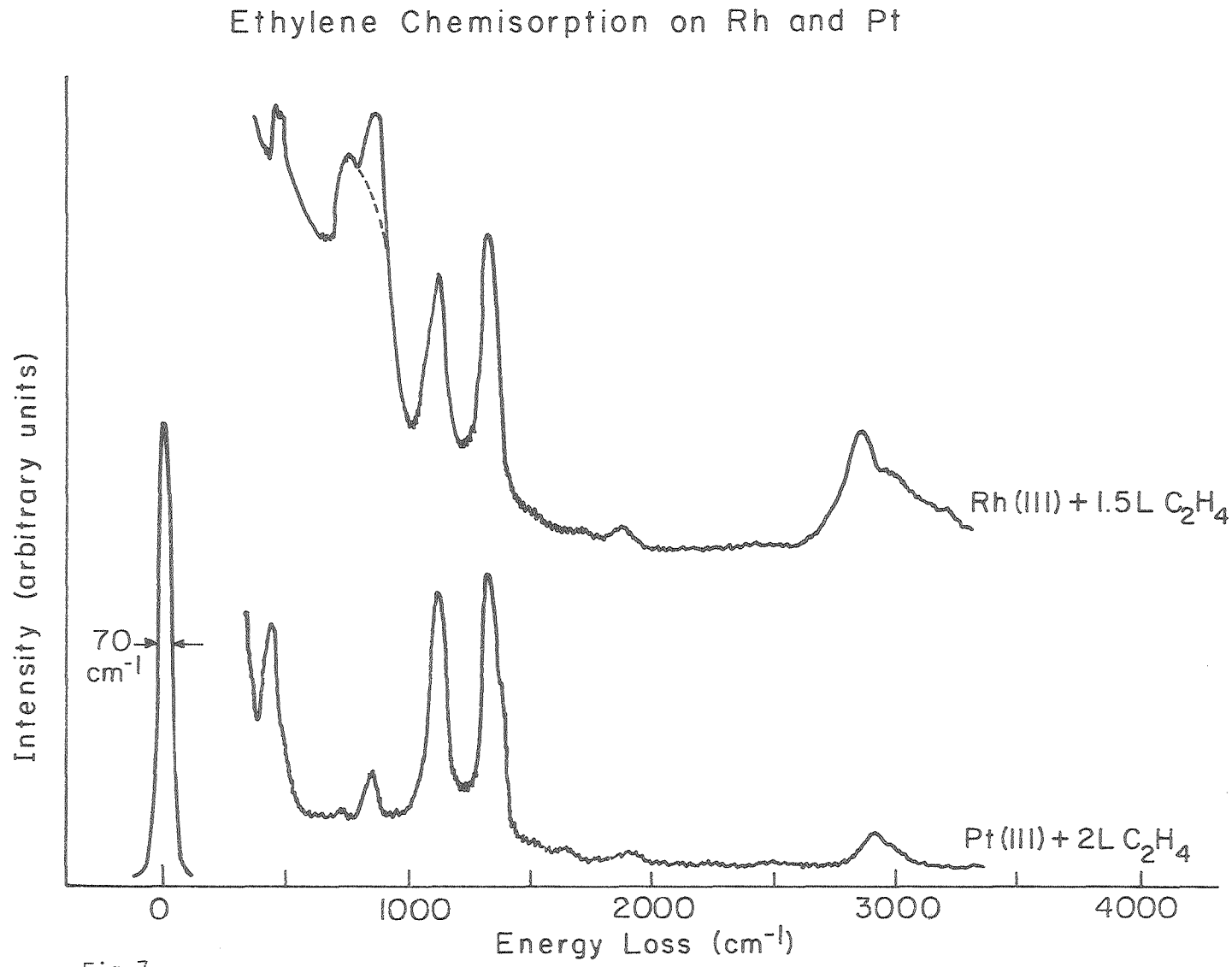


Fig.7

XBL7911-7290

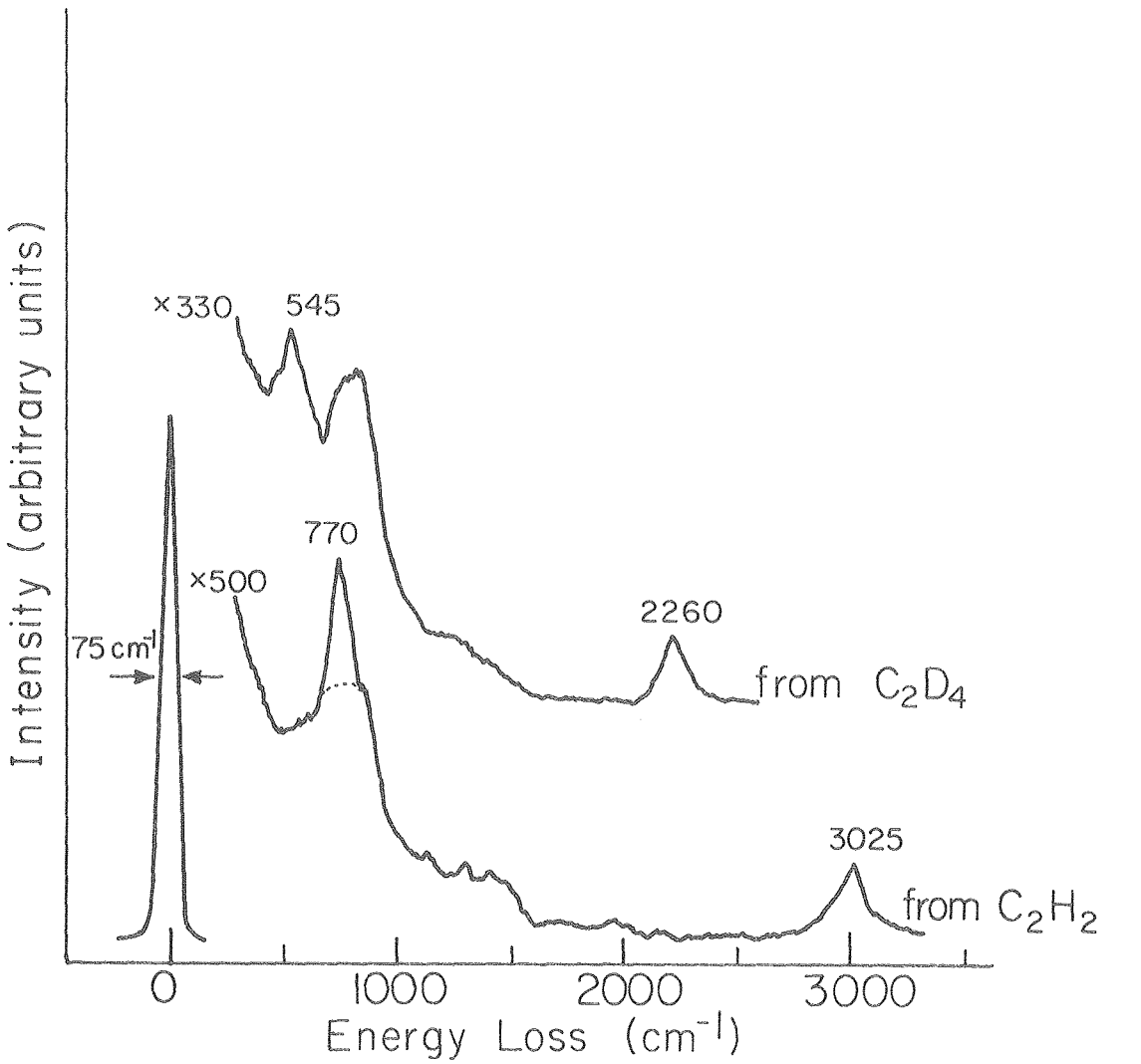


XBL 798-6970

Fig.8